Electronic Supplementary Material (ESI) for New Journal of Chemistry.

Bridged *o*-carborane-anthracene dyads as dual state emission luminogens: synthesis, characterization, and mechanochromic property

Chunyue Xu[a], Tianrui Li[a], Jinling Miao*[b], Kexin Liu[b], Yong Nie*[a], Guangning Liu[b], Xuchuan Jiang*[a,c]

[a]Institute for Smart Materials & Engineering, University of Jinan, No. 336 Nanxinzhuang West Road, 250022 Jinan, P. R. China
[b]School of Chemistry and Chemical Engineering, Shandong Provincial Key Laboratory of Fluorine Chemistry and Chemical Materials, University of Jinan, 250022 Jinan, P. R. China
[c]School of Materials Science and Engineering, University of Jinan, 250022 Jinan, P. R. China

Contents

Experimental section

Standard Schlenk techniques were used for the synthetic reaction under Ar. The solvents were commercially available and used without further purification. IR spectra were recorded in the range 450-4000 cm^{-1} on a Perkin Elmer Tensor II spectrometer using KBr pellets. ^{1}H- and ^{13}C-NMR analyses were performed using a Bruker Avance III 600 MHz spectrometer. As internal references for ^{1}H- and ^{13}C-NMR spectroscopy the signals of $CDCl_3$ were used and calculated relative to tetramethylsilane (TMS). ^{11}B-NMR spectrum was recorded in dichloromethane solutions (D_2O was added for locking) on a Bruker AVANCE III 500 spectrometer. Melting points were measured with a SGW X-4 apparatus and are not corrected. The high resolution mass spectrum was measured with a Thermo Scientific Q Exactive HF Orbitrap-FTMS instrument (AP-MALDI positive ion mode). UV-Vis spectra were recorded using a UV-9000S spectrometer. Emission spectra were measured with an Edinburgh FLS920 fluorimeter using a front-face solid sample configuration for solid samples. Absolute fluorescence quantum yields were obtained using an integrating sphere.

Synthesis of compound 2

Under argon atmosphere, compound **1** (80.1 mg, 0.23 mmol) was added into a Schlenk flask, cooled in ice-water bath, and sodium borohydride (18.9 mg, 0.50 mmol; added in three batches) and 30 mL of cold THF (kept in the refrigerator for about 3 h), and stirred to produce a yellow solution. After 30 min, the ice-water bath was removed and the solution was stirred at room temperature for 30 min, which turned pale yellow. After cooling in ice-water bath again, it was quenched the reaction with dilute hydrochloric acid (30 mL, 1 $mol \cdot L^{-1}$). The aqueous phase was extracted with dichloromethane (20 mL × 5), the organic phases were combined, dried with anhydrous sodium sulfate, filtered, and the filtrate was dried under reduced pressure to obtain a crude product, which was separated by preparative thin layer chromatography (eluent *n*-hexane/dichloromethane = 2/1, *V*/*V*) to obtain the pale yellow solid **2**.

2: 71.6 mg, yield: 89.2%; R_f = 0.70 (*n*-hexane: dichloromethane = 2: 1, *V*/*V*); m.p. 185.5 °C; IR (KBr): υ = 3361 (N-H), 3060, 2920 (C-H), 2586 (B-H), 1453, 1260 (C-N), 1071, 885, 728 cm^{-1}; ^{1}H-NMR (600 MHz, $CDCl_3$): δ = 8.47 (s, 1H, ArH), 8.11 (d, *J* = 8.9 Hz, 2H, ArH), 8.03 (d, *J* = 8.4 Hz, 2H, ArH), 7.62 ~ 7.55 (m, 2H, ArH), 7.53 ~ 7.47 (m, 2H, ArH), 4.93 (s, 2H, CH_2), 3.96 (s, 1H,

$C_{cage}H$), 2.93 (s, 1H, NH); ^{13}C NMR (151 MHz, $CDCl_3$): δ = 131.41, 130.18, 129.39, 128.67, 127.02, 126.91, 125.25, 123.02, 93.79, 69.33, 45.47; ^{11}B NMR (128 MHz, CH_2Cl_2) δ -3.24 (1B), -10.10 (1B), -11.55 (4B), -13.47 (2B), -14.21 (2B); MALDI-MS: *m/z* (%): calcd. for $C_{17}B_{10}H_{23}N$, 351.2756 $[M]^+$, found 351.2749.

Table S1 Crystal data and structure refinement for **2**

Empirical formula	$C_{68}H_{92}B_{40}N_4$
Formula weight	1397.85
Temperature/K	293
Crystal system	orthorhombic
Space group	$Pna2_1$
a/Å	24.8057(6)
b/Å	15.1639(4)
c/Å	21.0939(6)
α/°	90
β/°	90
γ/°	90
Volume/$Å^3$	7934.5(4)
Z	4
$\rho_{calc}g/cm^3$	1.170
μ/mm^{-1}	0.060
F(000)	2912.0
Crystal size/mm^3	0.65 × 0.44× 0.41
Radiation	MoKα (λ = 0.71073)
2Θ range for data collection/°	7.00 to 54.12
Index ranges	$-26 \le h \le 30$, $-18 \le k \le 18$, $-25 \le l \le 25$
Reflections collected	65154
Independent reflections	14730 [R_{int} = 0.0462, R_{sigma} = 0.0405]
Data/restraints/parameters	14730/1/1009
Goodness-of-fit on F^2	1.013
Final R indexes [I>=2σ (I)]	R_1 = 0.0686, wR_2 = 0.1613
Final R indexes [all data]	R_1 = 0.1145, wR_2 = 0.1947
Largest diff. peak/hole / e $Å^{-3}$	0.26/-0.25
CCDC deposition number	2160410

Table S2 Selected bond lengths and torsion angles for **2**

bond lengths (Å)		bond angles [°]		torsion angles [°]	
C1-C2	1.707 (8)	C1-C2-N1	120.9 (5)	C1-C2-N1-C3	-59.81
C2-N1	1.408 (6)	C2-N1-C3	120.1 (4)	C2-N1-C3-C4	-170.15
N1-C3	1.453 (6)	N1-C3-C4	111.9 (5)	N1-C3-C4-C5	89.57
C3-C4	1.528 (8)	C3-C4-C5	119.7 (6)	N1-C3-C4-C17	-94.44
C4-C5	1.411 (10)	C3-C4-C17	119.4 (7)	C18-C19-N2-C20	104.62
C4-C17	1.404 (9)	C18-C19-N2	115.9 (4)	C35-C36-N3-C37	-103.18
C18-C19	1.722 (7)	C19-N2-C20	120.0 (4)	C52-C53-N4-C54	113.94
C19-N2	1.408 (6)	C35-C36-N3	116.8 (4)		
N2-C20	1.463 (6)	C36-N3-C37	119.7 (4)		
C35-C36	1.696 (7)	C52-C53-N4	119.1 (4)		
C36-N3	1.403 (6)	C53-N4-C54	120.5 (4)		
N3-C37	1.478 (6)				
C52-C53	1.704 (7)				
C53-N4	1.390 (6)				
N4-C54	1.462 (7)				

Reference for the Gaussian package for the DFT calculations:

M. J. Frisch, G. W. Trucks, H. B. Schlegel, G. E. Scuseria, M. A. Robb, J. R. Cheeseman, G. Scalmani, V. Barone, B. Mennucci, G. A. Petersson, H. Nakatsuji, M. Caricato, X. Li, H. P. Hratchian, A. F. Izmaylov, J. Bloino, G. Zheng, J. L. Sonnenberg, M. Hada, M. Ehara, K. Toyota, R. Fukuda, J. Hasegawa, M. Ishida, T. Nakajima, Y. Honda, O. Kitao, H. Nakai, T. Vreven, J. A. Montgomery, Jr., J. E. Peralta, F. Ogliaro, M. Bearpark, J. J. Heyd, E. Brothers, K. N. Kudin, V. N. Staroverov, R. Kobayashi, J. Normand, K. Raghavachari, A. Rendell, J. C. Burant, S. S. Iyengar, J. Tomasi, M. Cossi, N. Rega, J. M. Millam, M. Klene, J. E. Knox, J. B. Cross, V. Bakken, C. Adamo, J. Jaramillo, R. Gomperts, R. E. Stratmann, O. Yazyev, A. J. Austin, R. Cammi, C. Pomelli, J. W. Ochterski, R. L. Martin, K. Morokuma, V. G. Zakrzewski, G. A. Voth, P. Salvador, J. J. Dannenberg, S. Dapprich, A. D. Daniels, O. Farkas, J. B. Foresman, J. V. Ortiz, J. Cioslowski, and D. J. Fox, Gaussian 09, Revision A.02, Gaussian, Inc., Wallingford CT, 2009.

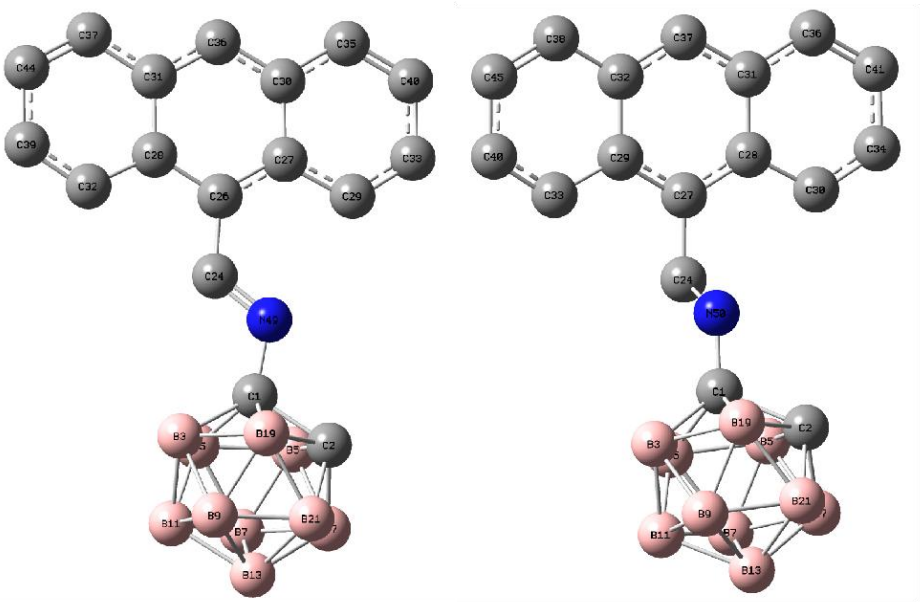

1 **2**

Fig. S1 Structures of **1** and **2** optimized at the B3LYP/6-31G (d,p) level of theory

Table S3 Selected bond lengths/angles and torsion angles of the optimized structures of **1** and **2**

Compounds	bond lengths (Å)		Bond angles [°]		torsion angles [°]	
1	C1-C2	1.648	C2-C1-N49	113.24	C2-C1-N49-C24	-177.55
	C1-N40	1.417	C1-N49-C24	118.49	C1-N49-C24-C26	-178.84
	N40-C24	1.287	N49-C24-C26	125.68	N49-C24-C26-C27	25.09
	C24-C26	1.465	C24-C26-C27	123.14	N49-C24-C26-C28	-157.80
	C26-C28	1.430	C24-C26-C28	116.70		
	C26-C27	1.429				
2	C1-C2	1.708	C1-C2-N50	115.47	C2-C1-N50-C24	125.44
	C1-N50	1.411	C1-N50-C24	119.87	C1-N50-C24-C27	117.80
	N50-C24	1.478	N50-C24-C27	110.03	N50-C24-C27-C28	85.17
	C24-C27	1.515	C24-C27-C28	119.87	N50-C24-C27-C29	-105.06
	C27-C28	1.416	C24-C27-C29	119.86		
	C27-C29	1.416				

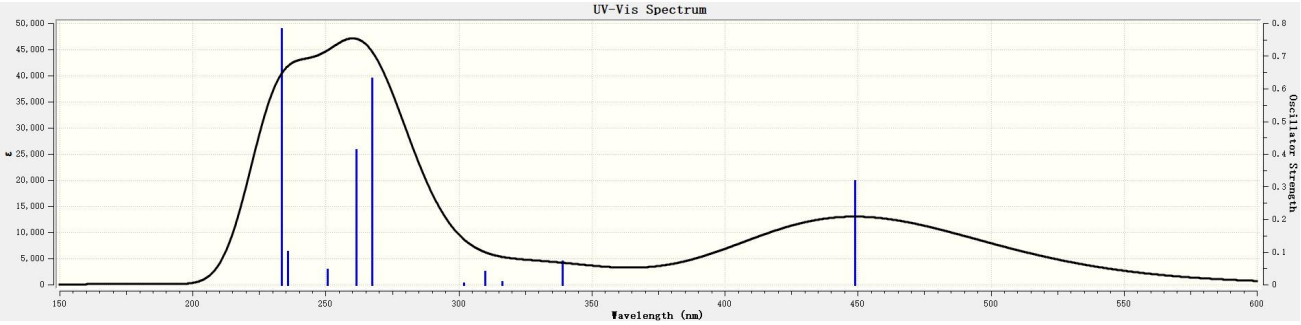

Fig. S2 Absorption spectrum of **1** in CH_2Cl_2 by DFT calculation

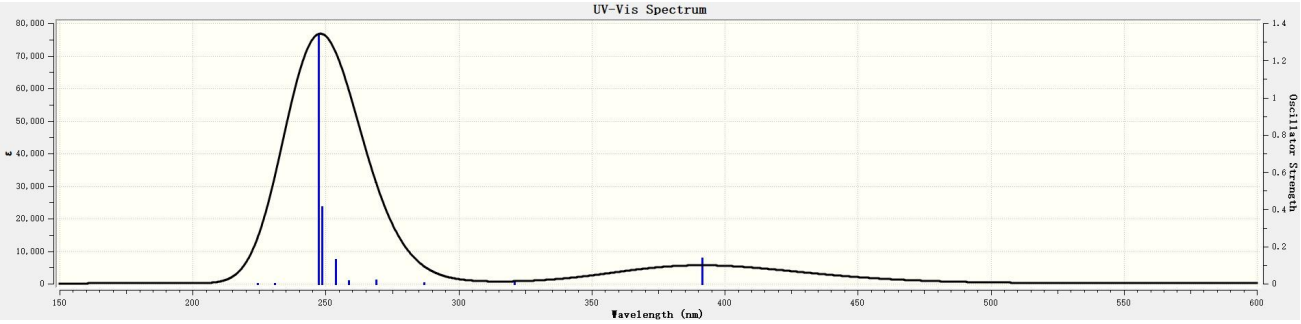

Fig. S3 Absorption spectrum of **2** in CH_2Cl_2 by DFT calculation

Table S4 Computed excitation energies and oscillator strengths for **1** from TD-DFT calculations in CH_2Cl_2[a]

state	E (ev)	λ (nm)	*f*	transitions
1	2.7617	448.95	0.3189	HOMO→LUMO (99.0%)
2	3.6582	338.92	0.0711	HOMO - 1→LUMO (75.5%)
				HOMO→LUMO + 2 (22.4%)
3	3.9200	316.28	0.0092	HOMO - 3→LUMO (10.8%)
				HOMO - 2→LUMO (85.7%)
4	4.000	309.96	0.0408	HOMO→LUMO + 1 (95.7%)
5	4.1068	301.90	0.0034	HOMO - 3→LUMO (84.0%)
				HOMO - 3→LUMO + 1 (2.1%)
				HOMO - 2→LUMO (11.2%)
6	4.6532	267.48	0.6324	HOMO - 4→LUMO (9.8%)
				HOMO - 1→LUMO (17.4%)
				HOMO - 1→LUMO + 1 (15.7%)
				HOMO→LUMO + 2 (54.6%)
7	4.7439	261.35	0.4132	HOMO - 4→LUMO (84.4%)
				HOMO - 1→LUMO + 1 (2.2%)
				HOMO→LUMO + 2 (5.8%)
8	4.9446	250.75	0.0454	HOMO - 2→LUMO + 1 (2.9%)
				HOMO→LUMO + 2 (2.0%)
				HOMO→LUMO + 3 (89.5%)

9	5.2615	235.64	0.1020	HOMO - 1→LUMO + 1 (11.7%) HOMO→LUMO + 2 (2.1%) HOMO→LUMO + 4 (79.6%)
10	5.3123	233.39	0.7832	HOMO - 3→LUMO + 1 (2.7%) HOMO - 2→LUMO + 1 (2.5%) HOMO - 1→LUMO(2.8%) HOMO - 1→LUMO + 1 (61.7%) HOMO→LUMO + 2 (11.0%)

[a] calculated at the B3LYP/6-31G (d,p) level of theory.

Table S5 Computed excitation energies and oscillator strengths for **2** from TD-DFT calculations in CH_2Cl_2[a]

state	E (ev)	λ (nm)	*f*	transitions
1	3.1666	391.54	0.1365	HOMO→LUMO (98.5%)
2	3.8632	320.94	0.0068	HOMO - 1→LUMO (56.6%) HOMO→LUMO + 1 (42.5%)
3	4.3226	286.83	0.0040	HOMO - 2→LUMO (89.9%) HOMO - 1→LUMO (3.4%) HOMO→LUMO + 1 (2.2%) HOMO→LUMO + 4 (2.2%)
4	4.6104	268.92	0.0192	HOMO - 3→LUMO (75.3%) HOMO→LUMO + 3 (9.5%) HOMO→LUMO + 4 (11.3%)
5	4.7944	258.60	0.0147	HOMO→LUMO + 2 (97.6%)
6	4.8877	253.67	0.1274	HOMO - 3→LUMO (8.8%) HOMO - 2→LUMO (4.2%) HOMO - 1→LUMO (3.0%) HOMO→LUMO + 1 (5.4%) HOMO→LUMO + 3 (73.8%) HOMO→LUMO + 4 (2.1%)
7	4.9869	248.62	0.4133	HOMO - 3→LUMO (12.5%) HOMO -1→LUMO (9.1%) HOMO→LUMO + 1 (14.7%) HOMO→LUMO + 4 (60.9%)
8	5.0149	247.23	1.3450	HOMO - 2→LUMO (4.5%) HOMO - 1→LUMO (25.8%) HOMO→LUMO + 1 (32.8%) HOMO→LUMO + 3 (12.8%) HOMO→LUMO + 4 (21.8%)

9	5.3698	230.89	0.0004	HOMO - 4→LUMO (45.4%) HOMO→LUMO + 5 (2.4%) HOMO→LUMO + 6 (3.4%) HOMO→LUMO + 7 (46.0%)
10	5.5257	224.38	0.0016	HOMO - 5→LUMO (21.4%) HOMO - 3→LUMO + 1 (8.3%) HOMO - 2→LUMO + 1 (41.6%) HOMO - 1→LUMO + 3 (7.0%) HOMO -1→LUMO + 4 (11.0%) HOMO→LUMO + 5 (3.2%) HOMO→LUMO + 9 (4.4%)

[a] calculated at the B3LYP/6-31G (d,p) level of theory.

Table S6. Emission lifetime data of solid samples

Compounds	τ_1(ns)	percent	τ_2 (ns)	percent	τ_3 (ns)	percent	τ(ns)
1	0.8416	81.49	1.7116	18.51			1.00
2[a]	0.3974	35.41	1.5566	58.59	5.9336	6.00	1.41
2[b]	7.0730	59.02	14.4062	40.98			10.08

a: λ_{em} = 448 nm; b: λ_{em} = 518 nm

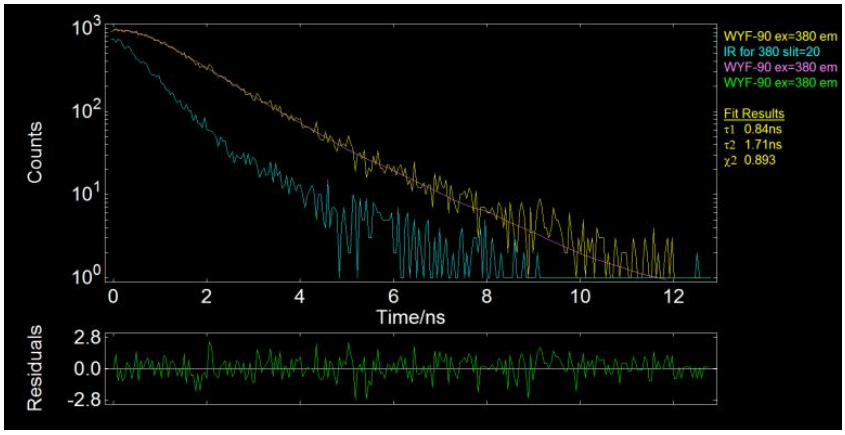

Fig. S4 PL decay curve of **1** (λ_{ex} = 380 nm, λ_{em} = 522 nm)

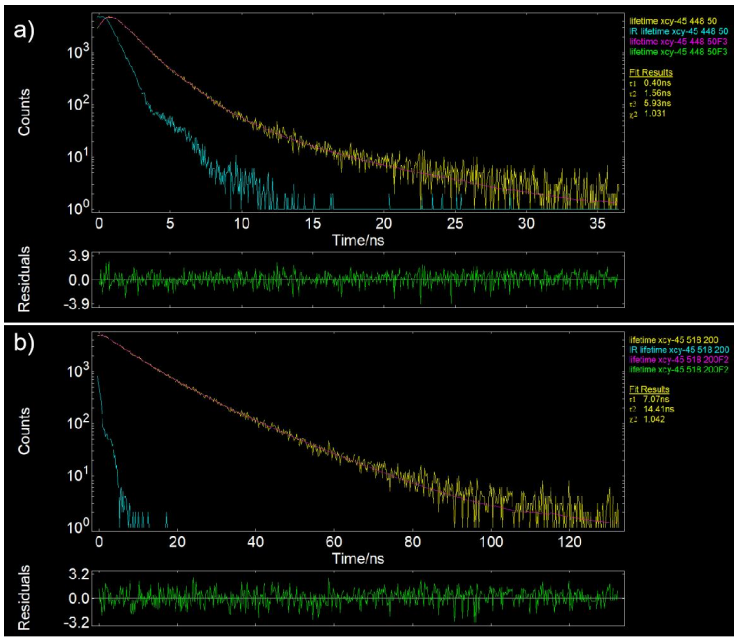

Fig. S5 PL decay curve of **2** (a): λ_{ex} = 380 nm, λ_{em} = 448 nm; b): λ_{ex} = 380 nm, λ_{em} = 518 nm)

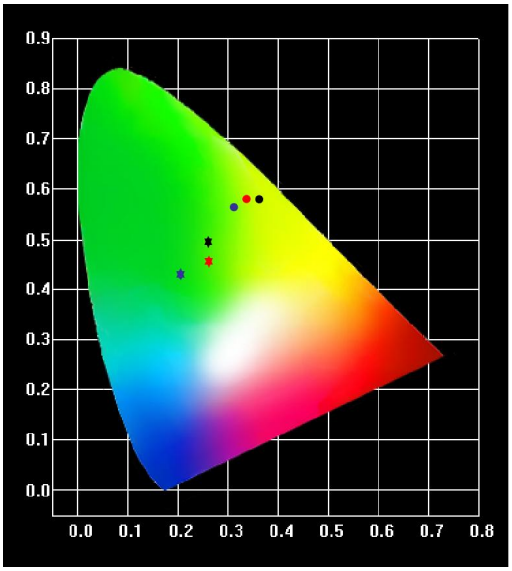

Fig. S6 CIE 1931 chromaticity diagram of **1** and **2** (solid circles represent **1** and pentacles represent **2**; powder: black; ground sample: blue; ground then annealed: red)

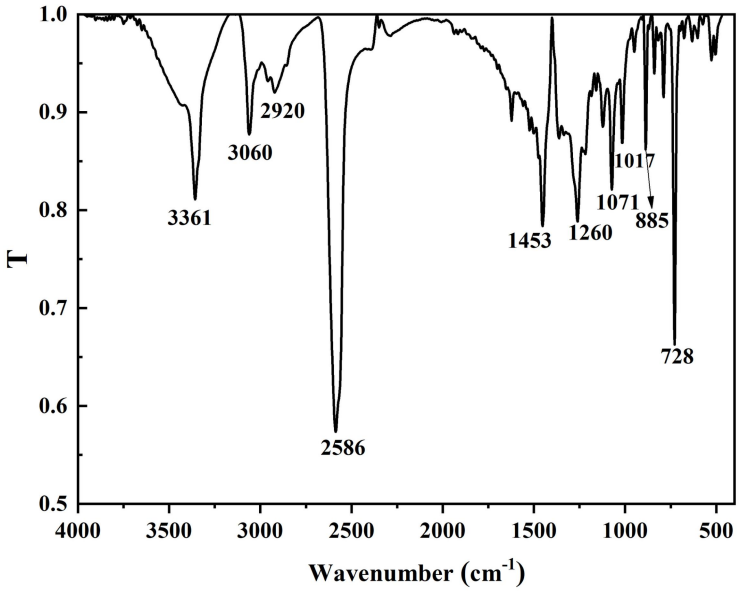

Fig. S7 FT-IR spectrum of **2** (KBr pellet)

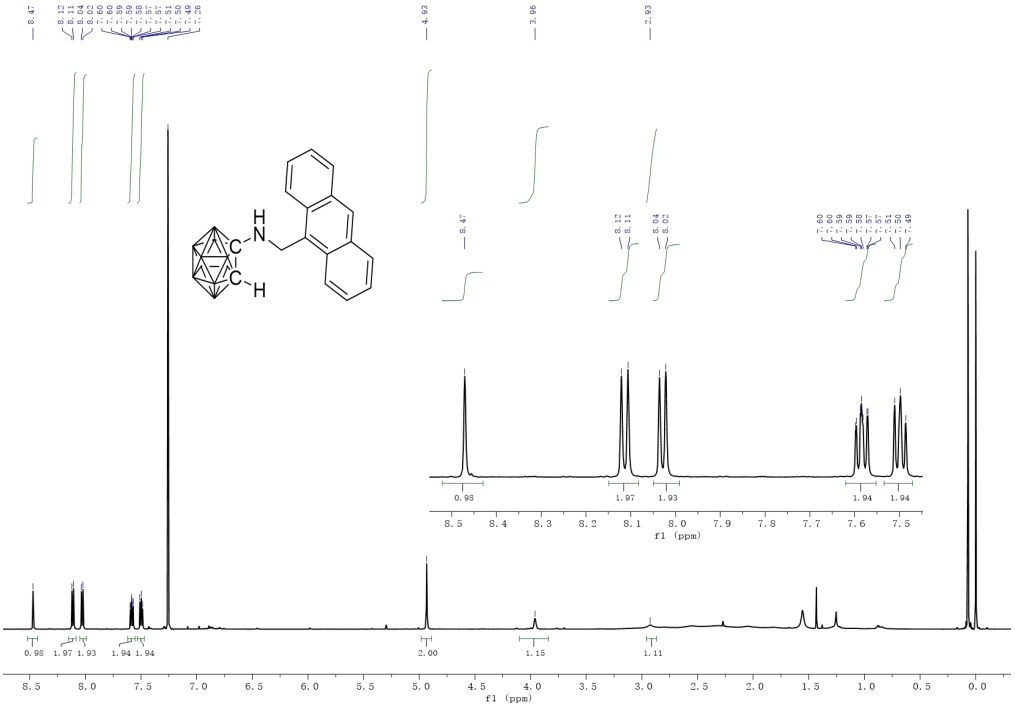

Fig. S8 ^{1}H-NMR spectrum of **2** in $CDCl_3$

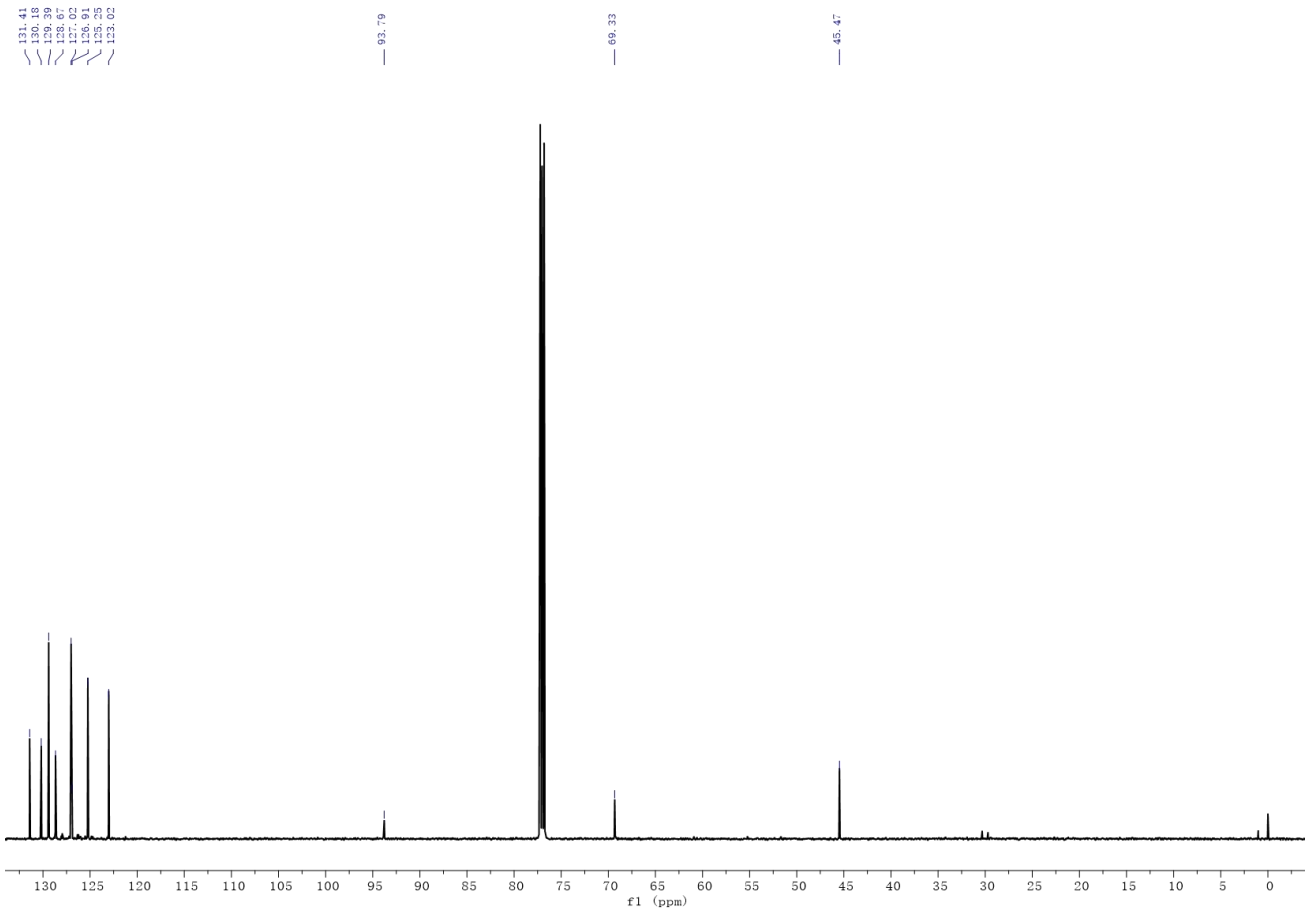

Fig. S9 ^{13}C-NMR spectrum of **2** in $CDCl_3$

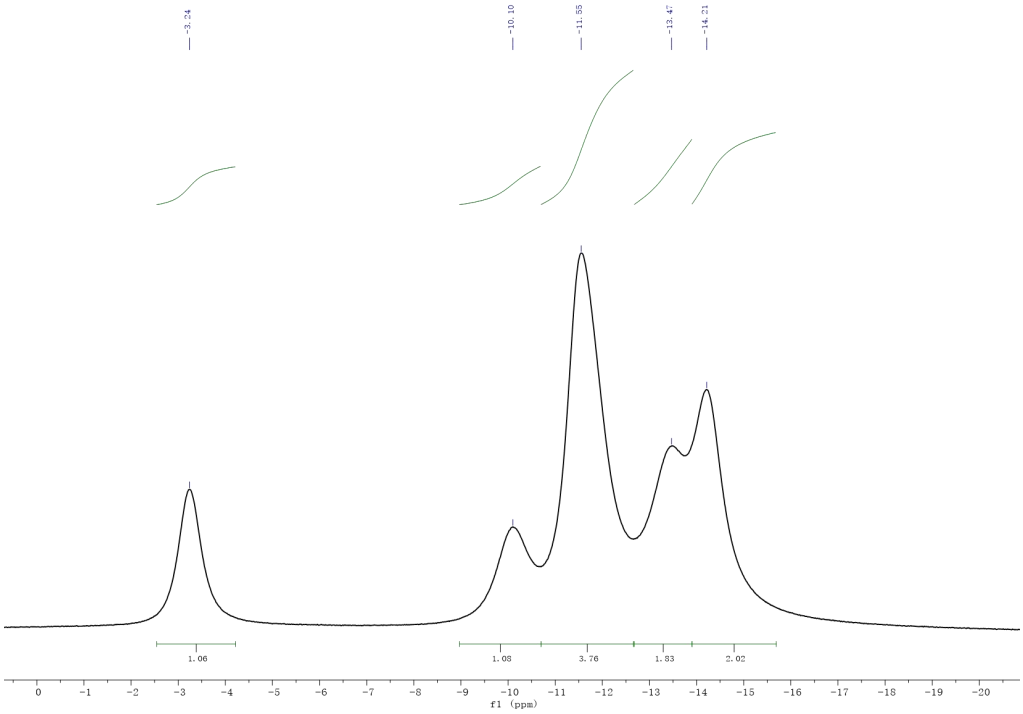

Fig. S10 ^{11}B{^{1}H}-NMR spectrum of **2** in CH_2Cl_2

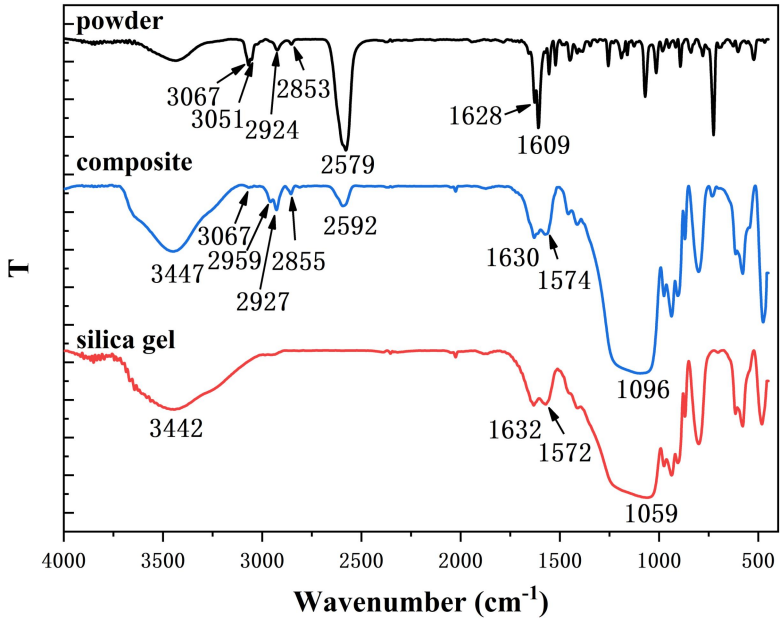

Fig. S11 FT-IR spectrum of the silica gel composite of **1**

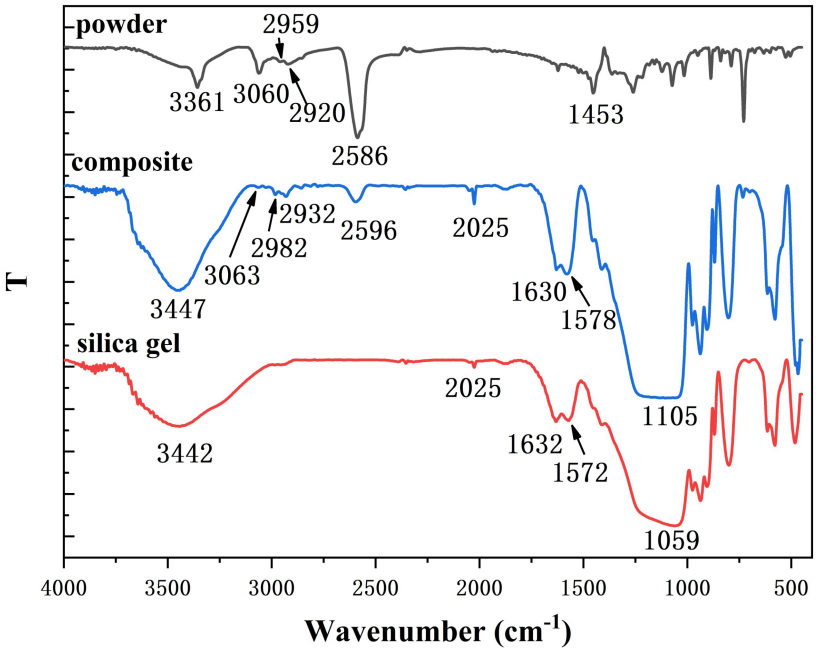

Fig. S12 FT-IR spectrum of the silica gel composite of **2**